



Effects of biodiesel, engine load and diesel particulate filter on nonvolatile particle number size distributions in heavy-duty diesel engine exhaust

Li-Hao Young^{a,*}, Yi-Jyun Liou^a, Man-Ting Cheng^b, Jau-Huai Lu^c, Hsi-Hsien Yang^d, Ying I. Tsai^e, Lin-Chi Wang^f, Chung-Bang Chen^g, Jim-Shoung Lai^a

^a Department of Occupational Safety and Health, China Medical University, 91, Hsueh-Shih Road, Taichung 40402, Taiwan

^b Department of Environmental Engineering, National Chung Hsing University, 250, Kuo-Kuang Road, Taichung 40254, Taiwan

^c Department of Mechanical Engineering, National Chung Hsing University, 250, Kuo-Kuang Road, Taichung 40254, Taiwan

^d Department of Environmental Engineering and Management, Chaoyang University of Technology, 168, Jifeng E. Road, Taichung 41349, Taiwan

^e Department of Environmental Engineering and Science, Chia Nan University of Pharmacy and Science, 60, Sec. 1, Erh-Jen Road, Tainan 71710, Taiwan

^f Department of Chemical and Materials Engineering, Cheng Shiu University, 840, Chengcing Road, Kaohsiung 83347, Taiwan

^g Fuel Quality and Engine Performance Research, Refining and Manufacturing Research Institute, Chinese Petroleum Corporation, 217, Minsheng S. Road, Chiayi 60036, Taiwan

ARTICLE INFO

Article history:

Received 23 June 2011

Received in revised form 2 November 2011

Accepted 3 November 2011

Available online 9 November 2011

Keywords:

Diesel engine exhaust

Nonvolatile particles

Number size distribution

Emission control technology

ABSTRACT

Diesel engine exhaust contains large numbers of submicrometer particles that degrade air quality and human health. This study examines the number emission characteristics of 10–1000 nm nonvolatile particles from a heavy-duty diesel engine, operating with various waste cooking oil biodiesel blends (B2, B10 and B20), engine loads (0%, 25%, 50% and 75%) and a diesel oxidation catalyst plus diesel particulate filter (DOC + DPF) under steady modes. For a given load, the total particle number concentrations (N_{TOT}) decrease slightly, while the mode diameters show negligible changes with increasing biodiesel blends. For a given biodiesel blend, both the N_{TOT} and mode diameters increase modestly with increasing load of above 25%. The N_{TOT} at idle are highest and their size distributions are strongly affected by condensation and possible nucleation of semivolatile materials. Nonvolatile cores of diameters less than 16 nm are only observed at idle mode. The DOC + DPF shows remarkable filtration efficiency for both the core and soot particles, irrespective of the biodiesel blend and engine load under study. The N_{TOT} post the DOC + DPF are comparable to typical ambient levels of $\sim 10^4 \text{ cm}^{-3}$. This implies that, without concurrent reductions of semivolatile materials, the formation of semivolatile nucleation mode particles post the aftertreatment is highly favored.

© 2011 Elsevier B.V. All rights reserved.

1. Introduction

Diesel engine has found widespread use in on-road vehicles and off-road equipments. However, its exhaust contains a number of hazardous air pollutants and large numbers of fine particles that have been linked to adverse health effects [1] and environmental impact [2,3]. Diesel engine particles (DEP) are a complex mixture of nonvolatile (or solid) and semivolatile components [4]. The nonvolatile component mainly consists of fractal-like carbonaceous

agglomerates also known as the accumulation (soot) mode in the size range of 30–500 nm [5]. Soot particles are formed in locally fuel-rich regions of the combustion flame in the engine. The semivolatile component is mainly composed of low- and semivolatile organic and sulfuric acid (H_2SO_4) vapors that originate from unburned fuel, lubricant oil, and partial combustion products [6,7]. Upon dilution and cooling in ambient air or during sampling, these vapors either condense on preexisting soot particles or nucleate to form nucleation mode particles in the size range of 3–30 nm. Such small sizes and the nonlinear nature of the nucleation pathway, in particular, have contributed largely to the measurement variability. On the other hand, a number of studies have shown the presence of nonvolatile cores in the nucleation mode particles [5,6,8–10]. Unlike the semivolatile nucleation mode particles that evaporate completely at temperature of 175 °C [11], these core particles could sustain under temperature of up to 450 °C. Considerations of the particle morphology, composition and volatility suggest that the cores are not derived from ash or sulfate but have composition similar to incipient soot particles or formed by pyrolyzed heavy hydrocarbon (HC) or oxidized metals in the

Abbreviations: B, biodiesel blend; CPC, condensation particle counter; DEP, diesel engine particles; DMA, differential mobility analyzer; DOC, diesel oxidation catalyst; DPF, diesel particulate filter; DR, dilution ratio; EGR, exhaust gas recirculation; ESC, European Steady Cycle; FSC, fuel sulfur content; HC, hydrocarbon; HDDE, heavy-duty diesel engine; PM, particulate matter; PMP, Particle Measurement Programme; RPD, relative percent difference; RSD, relative standard deviation; SMPS, scanning mobility particle sizer; SOF, soluble organic fraction; ThC, thermal conditioner; WCO, waste cooking oil.

* Corresponding author. Tel.: +886 4 2205 3366x6219; fax: +886 4 2207 5711.

E-mail address: lhy@mail.cmu.edu.tw (L.-H. Young).

engine. The above characteristics underscore the complexity and challenges in the measurement and interpretation of vapor–particle partitioning of DEP [12].

The occurrence, sizes and concentrations of the DEP depend on engine type, speed, load, fuel type, aftertreatment and sampling conditions. It is therefore important to exercise caution when comparing results from different studies. Nevertheless, general trends can be found and briefly provided in the following. As they are formed in the engine, the number and size of soot particles depend more on engine operating conditions and less on exhaust dilution and sampling [6]. Heavy-duty diesel engines (HDDE) typically emit higher particle number concentrations than spark-ignition engines and light-duty vehicles [13,14]. Higher speed and load are associated with an increase of number concentrations [14–16], particularly the soot particles [17–19]. Furthermore, the sizes of soot particles tend to increase with increasing load. Higher number concentrations of soot particles were observed while the exhaust gas recirculation (EGR) was operating [10,20,21]. Fuel sulfur content (FSC) has little effects on the soot number and size distribution (e.g., [17]). A number of studies have shown decreases of soot number and size with the use of biodiesels, originating from waste cooking oil (WCO) and methanol-biodiesel blends, with respect to Euro V and Euro 3 diesel vehicles [22,23]. The application of conventional diesel oxidation catalyst (DOC) has been shown to decrease particle mass by oxidizing the soluble organic fraction (SOF) but have little influence on the soot number and size [24].

The formation of semivolatile nucleation mode particles in engine exhaust has commonly been linked to the binary homogeneous nucleation of H_2SO_4 and H_2O [7,25] and possibly HC [26]. As such, the number concentrations of nucleation mode particles depend sensitively to temperature, dilution ratio (DR), humidity, FSC, soot number concentration, and aftertreatment. Typically, lower temperature, DR and soot number concentration favors enhanced nucleation [21,27]. Higher FSC also favors enhanced nucleation but the effects diminish when the FSC is < 50 ppmw [9,17]. A review by Lapuerta et al. [28] has reported that the majority of studies have shown increases of nucleation mode particle number concentration with biodiesel. The application of DOC or catalyzed diesel particulate filter (DPF) has been shown to promote the formation of semivolatile nucleation mode particles by enhancing the SO_2 -to- SO_3 conversion [6,26]. The nonvolatile cores in nucleation mode particles have been observed in light- and heavy-duty diesel engine exhaust at both low and high loads with regular, synthetic and biodiesel fuels [5,10,16,21]. Increasing number concentration of nonvolatile cores has been related to increasing load and injection pressure [29] and low soot particle numbers (e.g., EGR off). The nonvolatile core and soot particles are effectively removed by the DPF [10]; on the other hand, the filtration efficiency of semivolatile particles is less straightforward as they can be formed post the DPF.

The adverse impact of DEP has led to increasingly stringent particulate matter (PM) emission limits, in terms of particle mass. The resulting very low PM levels in engine exhaust pose significant challenges to the current gravimetric method, i.e., issues about the detection limit of microbalance and sampling artifact of semivolatile materials [30,31]. As a result, growing attention has been directed towards measurements of particle number concentration. Recently, the Working Party on Pollution and Energy of the United Nations Economic Commission for Europe Particle Measurement Programme (PMP) has developed a standard method for measuring the number concentration of non-volatile particles of diameters >23 nm, targeting the primary and aggregated soot particles [32]. This method has been shown to provide improved detection limit, accuracy, discrimination power, variability and reduced semivolatile artifact over the conventional gravimetric method [32,33]. Accordingly, the number-based emission limits

Table 1
Test engine specifications.

	Hino W06E
Year	1992
Configuration	In-line 6-cylinder
Air intake	Naturally aspirated
Fuel injection	Direct injection
Displacement	6.0 L
Max torque	412 Nm @ 1800 rpm
Max power	121 kW @ 3000 rpm
EGR	No

have been introduced in the Euro 5/6 regulation of light-duty vehicles and will be included in the Euro VI regulation of heavy-duty vehicles [34]. Such a change in methodology directly impacts how PM control technologies are evaluated and its subsequent implications in human and environment health need to be considered.

In Taiwan, the HDDE vehicles are of special interest because they contribute significantly (~50%) to the on-road $\text{PM}_{2.5}$ emission despite comprising only a small fraction of total vehicles [35]. Due to their long service life, ~24% of HDDE vehicles are of model year 1992 or older. In addition, the Taiwan EPA has required the recycling of WCO from the food manufacturing industry, fast food chains/restaurants, and domestic/school waste since 2007 [36]. The recovered WCO are mostly reused in the production of industrial/animal feedstock, soaps, and biodiesel. In a coordinated effort to save energy and reduce CO_2 emissions, the Bureau of Energy, Taiwan Ministry of Economic Affairs has mandated the addition of biodiesel into petroleum diesel since 2008. With that in mind, this study examines the effects of WCO biodiesel blends, along with varying engine load and the application of DOC + DPF, on the non-volatile particle number size distributions in HDDE exhaust. The present results are part of a larger collaborative research that aims to characterize the physicochemical and toxicological properties of DEP and to develop low-cost and high-efficiency aftertreatment devices. The chemical and toxicological characteristics of these DEP will be presented in subsequent publications.

2. Experimental methods

2.1. Test engines, cycles, fuels and diesel particulate filter

The experiments were conducted on a 6-cylinder, 6 L, naturally aspirated, water-cooled, no EGR, direct-injection HDDE of model year 1992 (Hino W06E). The detailed engine specifications are given in Table 1. The engine was certified to meet the Euro I emission standards. During the present study, the engine's PM emission factors at 0% load were in the range of $0.71\text{--}1.22\text{ g h}^{-1}$, while at 25% and 50% load were averaged in the range of $0.67\text{--}0.74\text{ g kW h}^{-1}$ without any aftertreatment. This relatively old engine model provides a more realistic challenge to the developed DOC + DPF because we focus on its "retrofit" application to in-use vehicles. The HDDE was tested with four out of the 13 European Steady Cycle (ESC) modes: mode 1, 3, 4 and 9. The average engine torque, speed and exhaust gas temperature for each test mode are given in Table 2. As shown, mode 1 (0% load) is idle, whereas the latter three test modes 9, 3 and 4 (25%, 50% and 75% load) represent engine operating with

Table 2
Engine test modes.

Load (%)	ESC mode	Torque (Nm)	Speed (rpm)	Exhaust T (°C)
0 (Idle)	1	–	750	76
25	9	98	1800	211
50	3	192	1800	324
75	4	293	1800	428

constant speed but varying torque. Therefore, this study primarily examines the effect of engine torque on particle emissions. For convenience in discussion, the four test modes are referred to as 0%, 25%, 50% and 75% load. The 100% load was not studied because the water recirculation cooling system would become overheated after a relatively short run time, thus preventing us from making representative aerosol measurements. The engine torque and speed were controlled by an engine dynamometer (Schenck W230). At the beginning and in-between test modes the engine was allowed a minimum of 3-min warm up time prior to aerosol measurements.

The base fuel was a petroleum low-sulfur (<50 ppmw) diesel without any addition of biodiesel (B0) from the Chinese Petroleum Corporation in Taiwan. However, the B0 is no longer available on the market as it has been blended with biodiesel since 2008. At the time of study in 2010, the market-available fuel already contains biodiesel content of 2% (B2), which is the baseline fuel in the present study. The B2 was further blended with neat WCO (B100) (Greatec Green Energy Co., Ltd.) by volume to 10% (B10) and 20% (B20) biodiesel blends. The B2 and B10 were not analyzed for fuel properties. Table 3 shows the fuel properties of the B0, B20 and B100.

The aftertreatment DOC+DPF under study is an active-type regeneration system. It consists of a DOC followed by a DPF with lengths of 10 cm and 30.5 cm, respectively, and the same outer diameter of 24 cm. The DOC and DPF both have a cell density of 100 cps, with each cell area of 0.2 cm × 0.2 cm, and cell thickness of 0.05 and 0.07 cm, respectively. The DOC is made of a ceramic straight-through honeycomb catalyzed with 1:1 mixture of platinum and palladium of 1 g m⁻³ loading. The DPF is an uncatalyzed ceramic wall-flow honeycomb with porosity of 45–50% and pore size of 2–3 μm. An expansion tube is connected between the exhaust pipe and the DOC+DPF to allow DEP diffuse evenly into the DOC+DPF. The measured back-pressure at 1500–2500 rpm is typically in the range of 1.5–2.5 kPa, and could reach above 4 kPa during DPF regeneration at 1200 rpm.

2.2. Sampling system and instrumentation

Fig. 1 shows the schematic diagram of the experimental set up and sampling system. It is noted that the DOC+DPF was always attached to the exhaust. Subsequently, two forward-facing L-shape sampling probes were placed upstream and downstream of the DOC+DPF to sample pre- and post-DOC+DPF exhaust, respectively. Aerosol sampling, dilution and thermal conditioning were carried out using a rotating disc thermo-dilution system that consists of a rotating disc dilutor (Matter Engineering Model MD19-2E) followed by a thermal conditioner (ThC, Matter Engineering Model ThC-1). The entire sampling process is described below. Engine exhaust was directly sampled with a peristaltic pump at a flow rate of ~1 L min⁻¹ (1pm). A ball valve was placed between the sampling

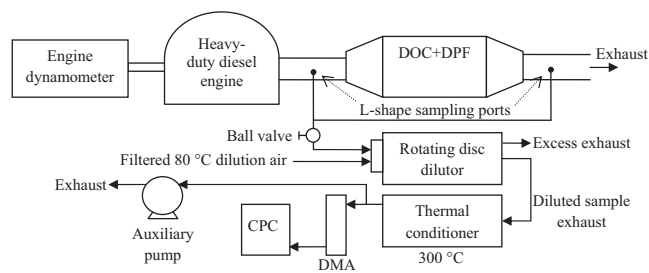


Fig. 1. Experimental set up and sampling system.

probe and the dilutor and was adjusted to provide exhaust flow rate of >~1 lpm, hence reducing the adverse effect of back pressure on the dilutor. A small fraction of sampled engine exhaust was then immediately mixed with filtered dilution air of 80 °C and ~1.5 lpm using a 10-cavity rotating disc. The dilution air flow rate was maintained by an auxiliary flow rate of ~1.2 lpm, plus the sample flow of 0.3 lpm drawn into the aerosol measurement instrument. By varying the disc rotation speed, DRs (i.e., the flow rate of dilution air divided by that of the sample air) in the range of 15–300 were achieved. The diluted sample was subsequently thermally conditioned at 300 °C in a thermally-insulated stainless steel tube of 25 cm length and 0.95 cm diameter to evaporate semivolatile materials that would otherwise condense on the diesel exhaust particles under ambient conditions. After thermal conditioning, the remaining aerosols are considered as nonvolatile or so-called “solid” particles. The number size distributions of diesel particles were then measured with a scanning mobility particle sizer and condensation particle counter (SMPS) system (GRIMM Model 5.500). The operating principles of the system are described in detail elsewhere [37]. In brief, the SMPS consists of a long Vienna-type differential mobility analyzer (L-DMA, GRIMM Model 55-900) and a butanol-based condensation particle counter (CPC, GRIMM Model 5.403). The detectable aerosol mobility diameters range from 11.1 to 1083.3 nm (44 size bins) with a sheath and sample flow rate of 3 lpm and 0.3 lpm, respectively. The saturator and condenser temperature of the CPC was set at 40 °C and 15 °C, respectively. The CPC has a 50% counting efficiency at 4.5 nm and measures number concentration up to 2 × 10⁴ cm⁻³ with single particle counting and coincidence correction, and up to 10⁷ cm⁻³ with the photometric mode. The SMPS was set to down-scan 3 min and 18 s from 10,000 to 5 V plus a wait-time 12 s, producing one particle number size distribution every 3.5 min. The DMA and CPC efficiencies were taken into account in the data acquisition and inversion software provided by the manufacturer (GRIMM 5.477 Version 1.35 Build 1). In the present study, a minimum of three samples were collected for each test mode.

According to the manufacturer, particle losses in the rotating disc dilutor are taken into account by the calibration factor for the stated DR. In addition, experimentally derived standard

Table 3
Fuel properties.

Fuel property	B0 ^a	B20	B100	ASTM
Density at 15 °C (g ml ⁻¹)	0.8386	0.8520	0.8805	D4052
Flash point (°C)	79	99	185	D93
Dynamic viscosity at 40 °C (cSt)	3.117	3.592	4.359	D445
Sulfur content (ppmw)	34.5	15	2.1	D2622
Polyaromatic content (wt%)	6	–	–	D6591
Total aromatic content (wt%)	28.2	–	–	D6591
Nitrogen content (wt%)	0.55	0.52	0.54	Elemental analysis
Carbon content (wt%)	84.95	82.39	75.87	Elemental analysis
Hydrogen content (wt%)	13.46	14.11	12.17	Elemental analysis
Gross heating value (cal g ⁻¹)	10259	9965	9516	D240

^a Petroleum low sulfur diesel.

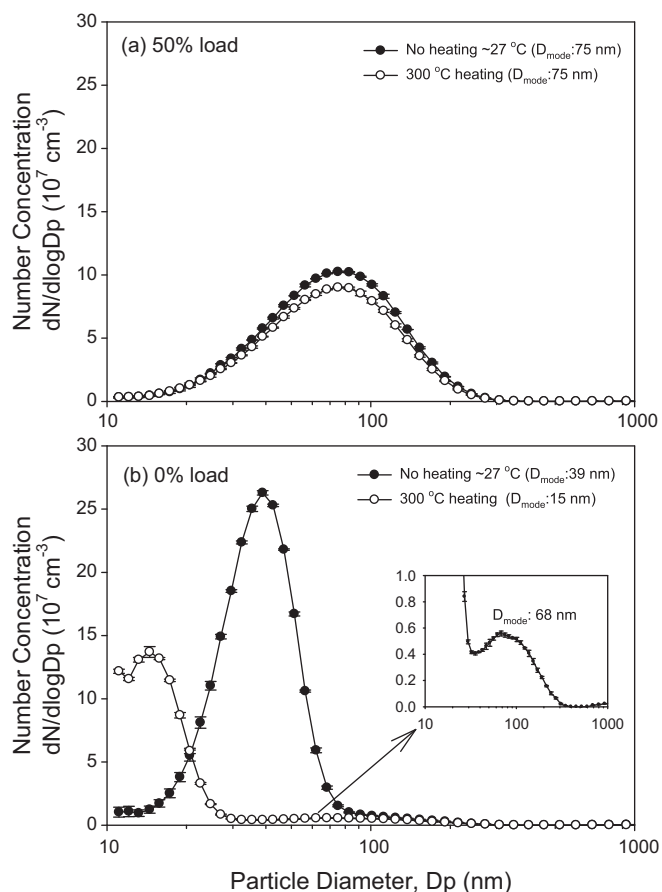


Fig. 2. Average particle size distributions in pre-DOC + DPF exhaust without ($\sim 27^\circ\text{C}$) and with thermal conditioning (300°C) at (a) 50% and (b) 0% load using B2.

values for losses with cold ThC are $\sim 3\%$ and with heated ThC are $\sim 15\%$. The latter thermophoretic losses were found to be in accordance with that of 12% determined in the present study with the HDDE running on B2 at 50% load (see Fig. 2a). The diffusion loss to the sample transfer lines between the exhaust and dilutor and between the ThC and SMPS (total length 1 m, flow rate 1.5 lpm and maximum exhaust temperature 430°C) was estimated to be $\sim 10\%$ for 10 nm particles [38]. We therefore did not make diffusion loss corrections to the measured concentration. Furthermore, the measured total particle number concentrations (N_{TOT} , i.e., 10–1000 nm particles) at 0% load under three different DR of 215, 250 and 300 showed that the relative percent differences (RPD) were $< 3\%$, with respect to DR = 300. The RPD for DR of 15, 17 and 19 tested at 25% load were $< 15\%$. Repeated measurements of N_{TOT} under various test modes on “single” days showed that the intra-variability, expressed as relative standard deviation (RSD), was in the range of 1–4%. Repeated measurements of N_{TOT} under various test modes on “different” days showed that the inter-variability was in the range of 4–18% RSD.

3. Results and discussion

In the following, all the presented N_{TOT} were corrected for dilution and refer to “nonvolatile” particles in the size range of 10–1000 nm. An exception is in the discussion of particle volatility where the N_{TOT} without thermal conditioning refers to “semivolatile” plus “nonvolatile” particles.

3.1. Volatility of diesel engine particles

The volatility of DEP was investigated by thermal conditioning the diluted DEP at 300°C prior to the number size distribution measurements. The HDDE was operated with B2 at 50% and 0% load. The measured average particle size distributions in pre-DOC + DPF exhaust without and with thermal conditioning are presented in Fig. 2. The error bars, in all figures, represent one standard deviation from repeated measurements. Without the thermal conditioning, the sample air temperature was $\sim 27^\circ\text{C}$. At 50% load, the measured particle mode diameter (D_{mode}) and N_{TOT} showed no practical changes after thermal conditioning; a persistent unimodal size distribution with D_{mode} of 75 nm was observed. This D_{mode} represents typical accumulation (soot) particles, composed primarily of carbonaceous agglomerates [12,13]. The identical D_{mode} with and without thermal conditioning indicates the nonvolatile characteristics of soot particles, as well as the low concentration of semivolatile HC in the exhaust of temperature $> 320^\circ\text{C}$ at medium or high load (Table 2). The decrease of N_{TOT} after thermal conditioning was only 12% due to diffusion and thermophoretic losses in the ThC, in line with that of 15% reported by the manufacturer. The lack of core or nucleation mode, with and without thermal conditioning, suggests the absence of re-nucleation of H_2SO_4 vapor in the present SMPS system. Nevertheless, as the lower size cut of the present SMPS system is 10 nm, it is unclear whether or not a core or nucleation mode of diameters < 10 nm was present in the exhaust. Using rapeseed methyl ester and low sulfur diesel, respectively, Heikkilä et al. [16] and Lähde et al. [21] have shown that high concentrations of nonvolatile cores of < 10 nm are present in HDDE exhaust at above 25% load.

At 0% load, the measured D_{mode} and N_{TOT} changed significantly after thermal conditioning. Without thermal conditioning, we observed a pronounced unimodal size distribution with D_{mode} of 39 nm. This particle mode at 39 nm, however, disappeared upon thermal conditioning and replaced by a pronounced nonvolatile core mode with D_{mode} of 15 nm, accompanied by a 57% reduction of N_{TOT} . The appearance of core mode after thermal conditioning was unlikely due to re-nucleation because the exhaust sample was considerably diluted with the DR ranging from 250–300. The observed substantial size reduction was due to thermal desorption of semivolatile materials condensed on the particles, e.g., the SOF. This is not surprising as higher HC concentrations, hence higher SOF values are typically associated at idle or light load because of incomplete combustion under lower combustion temperature (e.g., [24]). Rönkkö et al. [9] observed similar results though, unlike the present study, the measured N_{TOT} showed little changes after thermal conditioning. Here, the particle diffusion and thermophoretic losses ($\sim 12\%$) alone could not fully account for the observed N_{TOT} reduction of 57%. Taking the above together and considering the very small amount of soot particles (Fig. 2b inset), the results suggest that, without the thermal conditioning, the higher HC concentrations at 0% load may be responsible for not only particle growth but also enhanced nucleation. Earlier studies have shown that the formation of nucleation mode particles correlates well with the HC concentrations under low FSC, light load and without aftertreatment [9,26,39].

3.2. Effects of engine load

In this experiment, the HDDE was operated with B2 at 0% (idle), 25%, 50% and 75% load. The below results are similar to that using B10 and B20 (see Table 4) and hence not presented here. The measured nonvolatile N_{TOT} in pre-DOC + DPF exhaust at different engine loads using B2 are shown in Fig. 3. Also included in the figure are the N_{TOT} differences with respect to 25% load (baseline); 0% load was not used as the baseline because its particle

Table 4
The measured total nonvolatile particle number concentration (N_{TOT}) with different biodiesel blend and engine load.

Load (%)	B2	B10		B20	
	N_{TOT} (10^7 cm^{-3})	N_{TOT} (10^7 cm^{-3})	Reduction ^a (%)	N_{TOT} (10^7 cm^{-3})	Reduction ^a (%)
0	5.12	5.50	–7	3.44	33
25	3.13	2.37	24	1.89	40
50	4.97	3.92	21	3.27	34
Average	4.41	3.15	29 ^b	2.87	35

^a N_{TOT} reduction with respect to B2 for each engine load.

^b Excluding B10 at 0% load.

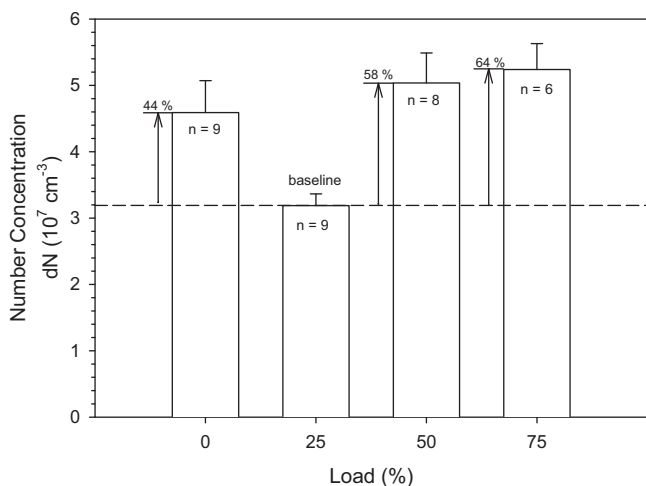


Fig. 3. The measured total nonvolatile particle number concentration (N_{TOT}) in pre-DOC + DPF exhaust at different engine loads using B2.

emission characteristics were substantially different from other test modes. The measured nonvolatile N_{TOT} ranged from 3.19×10^7 to $5.24 \times 10^7 \text{ cm}^{-3}$, which is slightly higher than that measured by Heikkilä et al. [16] who tested a HDDE with three different fuels at 25–100% load. It is notable that these concentrations are 10^3 times higher than typical ambient particle number concentration [40]. The nonvolatile N_{TOT} at 0% load were higher than at 25% load but lower than at 50% and 75% load. The N_{TOT} increased with increasing load from 25%, 50% to 75%, resulting a concentration increase of up to 64%. The measured nonvolatile size distributions in pre-DOC + DPF exhaust at different engine loads using B2 are shown in Fig. 4. The size distributions at 0% load were very different from

other test modes and exhibited bimodal, showing a predominant core mode of 15 nm and a substantially minor soot mode of ~ 68 nm. At above 25% load, the core mode disappeared. Instead, the size distributions were unimodal with a soot mode that increased in concentration and size with increasing load from 25%, 50% to 75%. The soot concentration increase is in accordance with Heikkilä et al. [16], but the size increase is not. Tzamkiozis et al. [41] have shown very similar unimodal particle size distributions between ~ 10 and 300 nm, without the core mode, from a diesel passenger car running on various biodiesels at constant speed of 50 km h^{-1} . Tsolakis [42] suggested that more soot particles are produced at higher load as a result of increased fuel consumption, smaller air-to-fuel ratio, longer period of diffusion combustion, and lower soot oxidation rate. The elevated numbers of soot particles in turn resulted in enhanced particle growth by coagulation.

3.3. Effects of waste cooking oil biodiesel

The measured nonvolatile N_{TOT} with the HDDE operated with three different WCO biodiesel blends and loads are given in Table 4. Also included in the table are the N_{TOT} reductions for each load with respect to B2. The N_{TOT} at a given load clearly showed a consistent and gradual reduction with increasing WCO biodiesel blend, with the exception of B10 at 0% load. Excluding that exceptional case, an increase of WCO biodiesel blend from 2% to 20% resulted in an overall N_{TOT} reduction of 35%. Fig. 5 shows the nonvolatile particle size distributions in pre-DOC + DPF exhaust at different loads using B2, B10 and B20. At 0% load, the number of core particles decreased with increasing biodiesel blend. At 25% and 50% load, the number of soot particles decreased with increasing biodiesel blend. Therefore, the number reduction with increasing biodiesel blend was not limited to soot particles but also included the core particles. This is likely due to the increased oxygen content, lower aromatic content, prolonged soot oxidation time, and lower final boiling point with increasing biodiesel blend [28,43]. The reduction of nonvolatile core particles, shown here, is more straightforward than the semivolatile nucleation mode particles, which have been shown by a majority of studies to increase with increasing biodiesel blend [28].

The D_{mode} changes of the nonvolatile core and soot particles were not considered significant (<6 nm) among different biodiesel blends. This suggests that biodiesel blend in between 2% and 20% have little or negligible effect on the nonvolatile particle size distribution. Using the same source of WCO, Lin et al. [44] have shown the HC concentration decreases with increasing WCO biodiesel blends from 5% to 30%. This indicates that particle growth due to HC condensation would likely be more preferable at lower biodiesel blends. It is therefore expected that, without thermal conditioning, the resulting semivolatile particle size distribution would show decreasing D_{mode} with increasing biodiesel blend at idle or low load. Without thermal conditioning, Lapuerta et al. [45] have shown the number-derived particle mass concentration and mean diameter decreased with increasing WCO biodiesel blends. Similarly, Di et al. [18] also reported a size reduction of soot particles with increasing

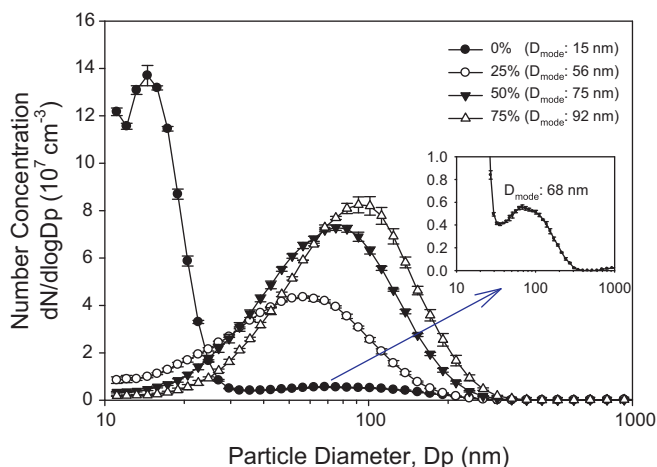


Fig. 4. Average nonvolatile particle size distributions in pre-DOC + DPF exhaust at different engine load using B2.

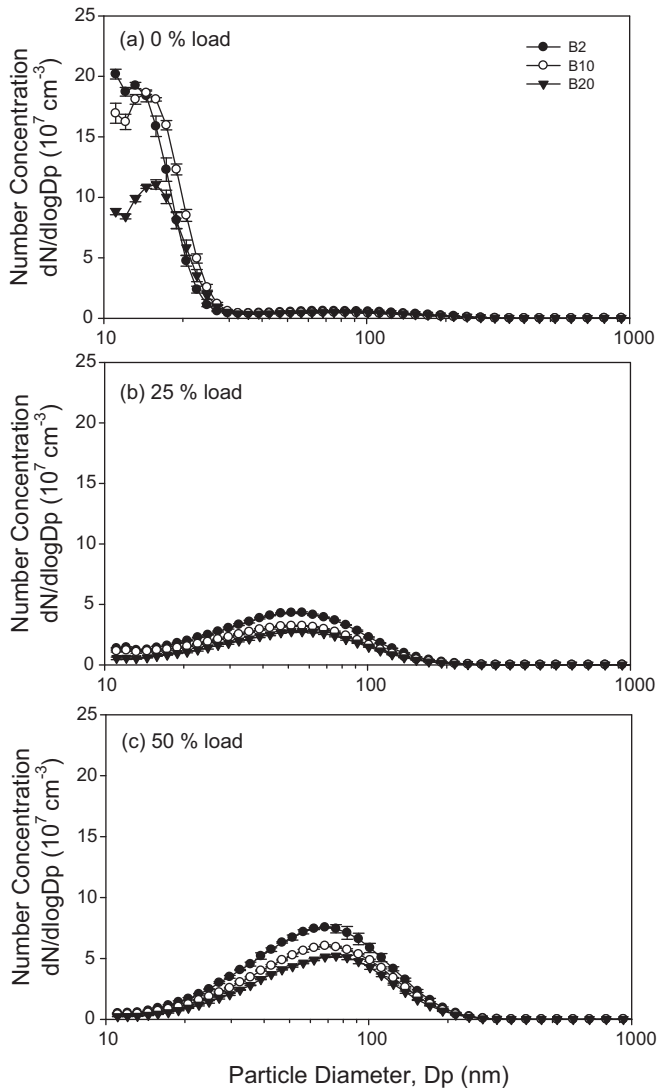


Fig. 5. Average nonvolatile particle size distributions in pre-DOC + DPF exhaust at (a) 0%, (b) 25% and (c) 50% load using B2, B10 and B20.

WCO biodiesel blend, though the total semivolatile particle concentration increased. The authors attributed the size reduction to the increase of oxygen (biodiesel) content in the fuel. As the previous two studies have tested the WCO biodiesel blends in a much wider range of 20–80%, it is also likely that the size reduction would not be observed when the blends are <20%. The present study focused on low concentrations of biodiesel blends because they are more likely to be the ones used in full-scale applications in the near future.

3.4. Efficiency of diesel particulate filter

The filtration efficiency of the DOC + DPF was tested with the HDDE operated with three different biodiesel blends and loads. Fig. 6 shows the measured nonvolatile N_{TOT} in pre-DOC + DPF and post-DOC + DPF exhaust at different loads using B2, B10 and B20. The results show that the nonvolatile particles were effectively removed by the DOC + DPF, with the filtration efficiencies >99.84% regardless of the biodiesel blend and load under study. Fig. 7 shows the average nonvolatile particle size distributions in post-DOC + DPF exhaust under different load and biodiesel blend. When examining the post-DOC + DPF size distributions, it is important to keep in mind that some of the N_{TOT} are very low and comparable

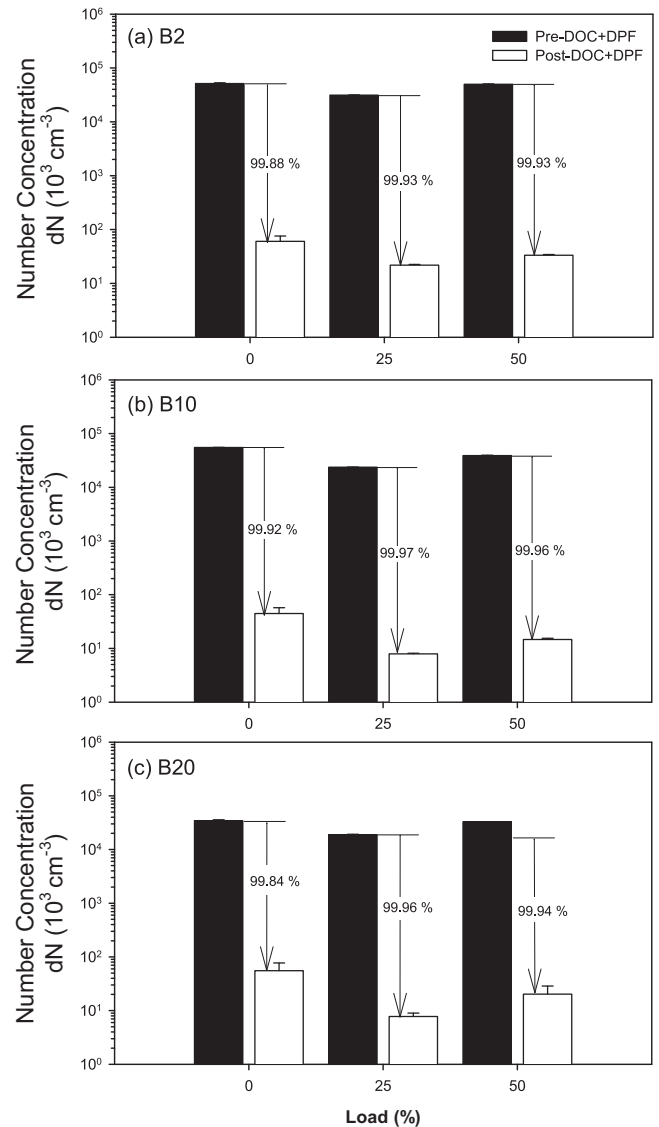


Fig. 6. Measured total nonvolatile particle number concentrations (N_{TOT}) in pre-DOC + DPF and post-DOC + DPF exhaust at various engine loads using (a) B2, (b) B10 and (c) B20.

to the ambient particle number level, i.e., $\sim 10^4 \text{ cm}^{-3}$. Such low concentrations give rise to increased measurement uncertainty, which is particularly large for >300 nm particles. These large particles, however, only contribute to <0.3% of N_{TOT} in most cases. As a result, measurement errors leading to unusual “spikes” in the post-DOC + DPF size distributions cannot be ruled out. Nevertheless, in comparison to Fig. 5, Fig. 7 indicates that the size distribution “modal” characteristics in pre-DOC + DPF exhaust remained practically unchanged after passing through the DOC + DPF. This is mainly due to the nearly equal, high filtration efficiencies across the particle-mode size range. The above results are in good agreement with that of De Filippo and Maricq [10], who investigated the effects of exhaust aftertreatment at idle condition and engine EGR off. The present study has extended the filtration efficiency tests to different WCO biodiesel blends and engine load. Biswas et al. [46] also showed little alteration of nonvolatile particle size distributions post the DOC + DPF (with continuous regenerating technology) using a thermodenuder at 230 °C, whereas a pronounced semivolatile nucleation mode was observed at lower temperature of 150 °C. In the present study, the DR was decreased

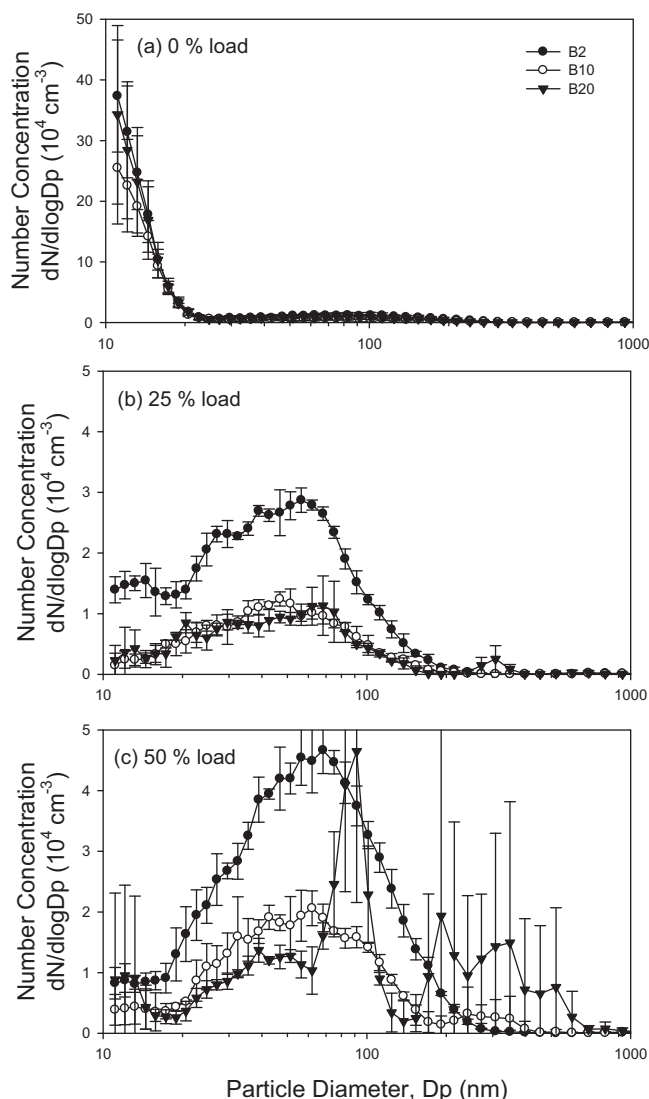


Fig. 7. Average nonvolatile particle size distributions in post-DOC + PDF exhaust at (a) 0%, (b) 25% and (c) 50% load using B2, B10 and B20. Note that the y-axis scale for the 0% load is 10 times higher than the others.

from above 250 to 15 to accommodate the low N_{TOT} . With that in mind, the persistence of nonvolatile core particles post the DOC+DPF suggests that the core particles observed at 0% load were not sampling artifact. In addition, the role of DOC in the particle number reduction and size alteration has been shown to be relatively negligible or minor [10,24,47]. Therefore, given that the test engine is a relatively old model with minimum control technologies, the above results underscore the highly effectiveness of DPF alone for nonvolatile particle number reduction. However, such efficiencies should not be mistaken as the same for the semivolatile nucleation mode particles, which could form post the aftertreatments as shown in previous studies [24,46,47]. If the nonvolatile particle reductions were not accompanied with concurrent reductions of semivolatile materials, the formation of semivolatile nucleation mode particles via homogeneous nucleation is highly favored under typical ambient conditions. This would in turn compromise the particle number filtration efficiencies of DPF. Bugarski et al. [47] have shown elevated nucleation mode particles post the DPF, resulting in low or even negative particle number filtration efficiencies.

4. Conclusions

The present study investigated the effects of biodiesel blend, engine load and DOC+DPF on the nonvolatile particle number emission characteristics in HDDE exhaust. The particle number size distributions were measured with a rotating disc thermo-dilutor system that provides hot dilution of 80 °C, DR ranging from 15 to 300 and thermal conditioning of diluted DEP at 300 °C. The results show that the nonvolatile N_{TOT} in HDDE exhaust increase with increasing load from 25% to 75%. On the other hand, the N_{TOT} decrease with increasing WCO biodiesel blends from 2% to 20%. The nonvolatile particle size distributions show a modest increase of mode diameters when increasing the engine load, whereas a negative or negligible effect on the mode diameters when increasing the WCO biodiesel blends. At 0% load (idle), the N_{TOT} are highest and the respective size distributions are strongly affected by condensation of semivolatile materials. At 0% load, thermal conditioning the DEP at 300 °C reveals nonvolatile core particles of <16 nm that would otherwise be identified as accumulation (soot) particles of 39 nm under ambient temperature. The DOC+DPF shows remarkable filtration efficiency for both the nonvolatile core and soot particles and had negligible effect on the size distributions, regardless of biodiesel blend and engine load under study. The DOC+DPF is very effective in reducing the numbers of nonvolatile component of the DEP to levels comparable to ambient concentrations of $\sim 10^4 \text{ cm}^{-3}$. Retrofitting such aftertreatment to in-use diesel vehicles shows great potential in meeting current nonvolatile particle number emission limits. However, it is important to note that the present measurements of nonvolatile particles are not representative of actual diesel particulate emissions, which contain both nonvolatile and semivolatile components. Furthermore, actual diesel emissions involve complex physical and chemical transformation upon cooling and dilution in ambient air. If the condensable vapors were not removed concurrently with the particles, the formation of semivolatile nucleation mode particles is highly favored upon exhaust cooling. With that in mind, the connection between the nonvolatile particle number methodology and the DEP-associated health risks needs to be additionally considered.

Acknowledgements

The financial and administrative support from the Taiwan EPA, National Science Council and China Medical University under the Contract# of NSC-98-EPA-M003-002, NSC-99-EPA-M-002-002 and CMU-97-250 are gratefully acknowledged. We would also like to thank Leder Company Ltd for technical support and assisting the study with an aerosol dilution system.

References

- [1] US EPA, Health Assessment Document for Diesel Engine Exhaust, National Center for Environmental Assessment, Office of Transportation and Air Quality, EPA/600/8-90/057F, 2002.
- [2] A. Eldering, G.R. Cass, Source-oriented model for air pollutant effects on visibility, *J. Geophys. Res.* 101 (1996) 19343–19369.
- [3] A.S. Ackerman, O.B. Toon, D.E. Stevens, A.J. Heymsfield, V. Ramanathan, E.J. Welton, Reduction of tropical cloudiness by soot, *Science* 288 (2000) 1042–1047.
- [4] H. Sakurai, K. Park, P.H. McMurry, D.D. Zarling, D.B. Kittelson, P.J. Ziemann, Size-dependent mixing characteristics of volatile and nonvolatile components in diesel exhaust aerosols, *Environ. Sci. Technol.* 37 (2003) 5487–5495.
- [5] D.B. Kittelson, W.F. Watts, J.P. Johnson, On-road and laboratory evaluation of combustion aerosols part 1: summary of diesel engine results, *J. Aerosol Sci.* 37 (2006) 913–930.
- [6] M.M. Maricq, R.E. Chase, N. Xu, P.M. Liang, The effects of the catalytic converter and fuel sulfur level on motor vehicle particulate matter emissions: light duty diesel vehicles, *Environ. Sci. Technol.* 36 (2002) 283–289.
- [7] J. Schneider, N. Hock, S. Weimer, S. Borrmann, U. Kirchner, R. Vogt, V. Scheer, Nucleation particles in diesel exhaust: composition inferred from in situ mass spectrometric analysis, *Environ. Sci. Technol.* 39 (2005) 6153–6161.

- [8] H. Sakurai, H.J. Tobias, K. Park, D. Zarling, K.S. Docherty, D.B. Kittelson, P.H. McMurry, P.J. Ziemann, On-line measurements of diesel nanoparticle composition and volatility, *Atmos. Environ.* 37 (2003) 1199–1210.
- [9] T. Rönkkö, A. Virtanen, J. Kannosto, J. Keskinen, M. Lappi, L. Pirjola, Nucleation mode particles with a nonvolatile core in the exhaust of a heavy duty diesel vehicle, *Environ. Sci. Technol.* 41 (2007) 6384–6389.
- [10] A. De Filippo, M.M. Maricq, Diesel nucleation mode particles: semivolatiles or solid? *Environ. Sci. Technol.* 42 (2008) 7957–7962.
- [11] H. Lüders, M. Krüger, P. Stommel, B. Lüers, The Role of Sampling Conditions in Particle Size Distribution Measurements, SAE Tech. Pap. Ser. 981374, 1998.
- [12] M.M. Maricq, Characterization of combustion and engine exhaust particles, in: J.C.M. Marijnissen, L. Gradoń (Eds.), *Nanoparticles in Medicine and Environment: Inhalation and Health Effects*, Springer Science + Business Media B.V., 2010.
- [13] D.B. Kittelson, Engines and nanoparticles: a review, *J. Aerosol Sci.* 29 (1998) 575–588.
- [14] D.C.S. Beddows, R.M. Harrison, Comparison of average particle number emission factors for heavy and light duty vehicles derived from rolling chassis dynamometer and field studies, *Atmos. Environ.* 42 (2008) 7954–7966.
- [15] J. Wang, J. Storey, N. Domingo, S. Huff, J. Thomas, B. West, Studies of diesel engine particle emissions during transient operations using an engine exhaust particle sizer, *Aerosol Sci. Technol.* 40 (2006) 1002–1015.
- [16] J. Heikkilä, A. Virtanen, T. Rönkkö, J. Keskinen, P. Aakko-Saksa, T. Murtonen, Nanoparticle emissions from a heavy-duty engine running on alternative diesel fuels, *Environ. Sci. Technol.* 43 (2009) 9501–9506.
- [17] Z.G. Liu, V.N. Vasys, D.B. Kittelson, Nuclei-mode particulate emissions and their response to fuel sulfur content and primary dilution during transient operations of old and modern diesel engines, *Environ. Sci. Technol.* 41 (2007) 6479–6483.
- [18] Y. Di, C.S. Cheung, Z. Huang, Comparison of the effect of biodiesel-diesel and ethanol-diesel on the particulate emissions of a direct injection diesel engine, *Aerosol Sci. Technol.* 43 (2009) 455–465.
- [19] Z.H. Zhang, C.S. Cheung, T.L. Chan, C.D. Yao, Experimental study on particulate emissions of a methanol fumigated diesel engine equipped with diesel oxidation catalyst, *Aerosol Sci. Technol.* 45 (2011) 262–271.
- [20] U. Mathis, M. Mohr, R. Kaegi, A. Bertola, K. Boulouchos, Influence of diesel engine combustion parameters on primary soot particle diameter, *Environ. Sci. Technol.* 39 (2005) 1887–1892.
- [21] T. Lähde, T. Rönkkö, A. Virtanen, A. Solla, M. Kytö, C. Söderström, J. Keskinen, Dependence between nonvolatile nucleation mode particle and soot number concentrations in an EGR equipped heavy-duty diesel engine exhaust, *Environ. Sci. Technol.* 44 (2010) 3175–3180.
- [22] L. Zhu, C.S. Cheung, W.G. Zhang, Z. Huang, Influence of methanol-biodiesel blends on the particulate emissions of a direct injection diesel engine, *Aerosol Sci. Technol.* 44 (2010) 362–369.
- [23] G. Fontaras, M. Kousoulidou, G. Karavalakis, T. Ztamkiozis, P. Pistikopoulos, L. Ntziachristos, E. Bakeas, S. Stournas, Z. Samaras, Effects of low concentration biodiesel blend application on modern passenger cars. Part 1: feedstock impact on regulated pollutants, fuel consumption and particle emissions, *Environ. Pollut.* 158 (2010) 1451–1460.
- [24] K. Vaaraslahti, J. Ristimäki, A. Virtanen, J. Keskinen, B. Giechaskiel, A. Solla, Effect of oxidation catalysts on diesel soot particles, *Environ. Sci. Technol.* 40 (2006) 4776–4781.
- [25] H.J. Tobias, D.E. Beving, P.J. Ziemann, H. Sakurai, M. Zuk, P.H. McMurry, D. Zarling, R. Waytulonis, D.B. Kittelson, Chemical analysis of diesel engine nanoparticles using a nano-DMA/thermal desorption particle beam mass spectrometer, *Environ. Sci. Technol.* 35 (2001) 2233–2243.
- [26] K. Vaaraslahti, A. Virtanen, J. Ristimäki, J. Keskinen, Nucleation mode formation in heavy-duty diesel exhaust with and without a particulate filter, *Environ. Sci. Technol.* 38 (2004) 4884–4890.
- [27] U. Mathis, J. Ristimäki, M. Mohr, J. Keskinen, L. Ntziachristos, Z. Samaras, P. Mikkanen, Sampling conditions for the measurement of nucleation mode particles in the exhaust of a diesel vehicle, *Aerosol Sci. Technol.* 38 (2004) 1149–1160.
- [28] M. Lapuerta, O. Armas, J. Rodríguez-Fernández, Effect of biodiesel fuels on diesel engine emissions, *Prog. Energy Combust. Sci.* 24 (2008) 198–223.
- [29] T. Lähde, T. Rönkkö, M. Happonen, C. Söderström, A. Virtanen, A. Solla, M. Kytö, D. Rothe, J. Keskinen, Effect of fuel injection pressure on a heavy-duty diesel engine nonvolatile particle emission, *Environ. Sci. Technol.* 45 (2011) 2504–2509.
- [30] J.J. Schauer, M.J. Kleeman, G.R. Cass, B.R. Simoneit, Measurement of emissions from air pollution sources. 1. C₁ to C₂₉ organic compounds from meat charbroiling, *Environ. Sci. Technol.* 33 (1999) 1566–1577.
- [31] E. Zervas, P. Dorlhène, L. Forti, C. Perrin, J.C. Momique, R. Monier, H. Ing, B. Lopez, Interlaboratory test of exhaust PM using ELPI, *Aerosol Sci. Technol.* 39 (2005) 333–346.
- [32] B. Giechaskiel, M. Cresnoverh, H. Jörgl, A. Bergmann, Calibration and accuracy of a particle number measurement system, *Meas. Sci. Technol.* 21 (2010), doi:10.1088/0957-0233/21/4/045102.
- [33] B. Giechaskiel, P. Dilara, J. Andersson, Particle Measurement Programme (PMP) light-duty inter-laboratory exercise: repeatability and reproducibility of the particle number method, *Aerosol Sci. Technol.* 42 (2008) 528–543.
- [34] B. Giechaskiel, M. Carriero, G. Martini, J. Andersson, Heavy Duty Particle Measurement Programme (PMP): Exploratory Work for the Definition of the Test Protocol, SAE Tech. Pap. Ser. 2009-01-1767, 2009.
- [35] TW EPA (Taiwan Environmental Protection Administration), Taiwan Emission Data System (TEDS) 7.1, http://ivy2.epa.gov.tw/air-ei/new_main2-0-1.htm, 2011 (accessed 2011/5/10).
- [36] TW EPA, Department of Waste Management, <http://waste.epa.gov.tw/>, 2011 (accessed 2011/9/1).
- [37] M. Heim, G. Kasper, G.P. Reischl, C. Gerhart, Performance of a new commercial electrical mobility spectrometer, *Aerosol Sci. Technol.* 38 (2004) 3–14.
- [38] P.A. Baron, K. Willeke, *Aerosol Measurement: Principles, Techniques, and Applications*, second ed., John Wiley and Sons, New York, 2001.
- [39] K. Vaaraslahti, J. Keskinen, B. Giechaskiel, A. Solla, T. Murtonen, H. Vesala, Effect of lubricant on the formation of heavy-duty diesel engine nanoparticles, *Environ. Sci. Technol.* 39 (2005) 8497–8504.
- [40] L. Morawska, Z. Ristovski, D.U. Jayaratne, X. Ling, Ambient nano and ultrafine particles from motor vehicle emissions: characteristics, ambient processing and implications, *Atmos. Environ.* 42 (2008) 8113–8138.
- [41] T. Ztamkiozis, L. Ntziachristos, A. Mamakos, G. Fontaras, Z. Samaras, Aerodynamic and mobility size distribution measurements to reveal biodiesel effects on diesel exhaust aerosol, *Aerosol Sci. Technol.* 45 (2011) 587–595.
- [42] A. Tsolakis, Effects on particle size distribution from the diesel engine operating on RME-biodiesel with EGR, *Energy Fuel* 20 (2006) 1418–1424.
- [43] J. Xue, T.E. Grift, A.C. Hansen, Effect of biodiesel on engine performances and emissions, *Renew. Sust. Energy Rev.* 15 (2011) 1098–1116.
- [44] Y.C. Lin, K.H. Hsu, C.B. Chen, Experimental investigation of the performance and emissions of a heavy-duty diesel engine fueled with waster cooking oil biodiesel/ultra-low sulfur diesel blends, *Energy* 36 (2011) 241–248.
- [45] M. Lapuerta, J. Rodríguez-Fernández, J.R. Agudelo, Diesel particulate emissions from used cooking oil biodiesel, *Bioresour. Technol.* 99 (2008) 731–740.
- [46] S. Biswas, S. Hu, V. Verma, J.D. Herner, W.H. Robertson, A. Ayala, C. Sioutas, Physical properties of particulate matter (PM) from late model heavy-duty diesel vehicles operating with advanced PM and NOx emission control technologies, *Atmos. Environ.* 42 (2008) 5622–5634.
- [47] A.D. Bugarski, G.H. Schnakenberg Jr., J.A. Hummer, E. Cauda, S.J. Janisko, L.D. Patts, Effects of diesel exhaust after treatment devices on concentrations and size distribution of aerosols in underground mine air, *Environ. Sci. Technol.* 43 (2009) 6737–6743.